Variation in seismic response of an embankment on liquefiable ground in dynamic centrifuge modeling

Yasuhiro Ikami, Katsutoshi Ueno & Ryosuke Uzuoka
Department of Civil and Environmental Engineering – Tokushima University, Tokushima, Japan

ABSTRACT
Centrifuge modeling is one of the most popular and reliable physical modeling method for geomaterials; therefore the results of centrifuge modeling have been used for validation process of newly developed numerical method including constitutive models of soil. However, uncertainties in centrifuge modeling have not been discussed in most validation cases of geotechnical problems although it was well known that geotechnical centrifuge modeling includes some uncertainties such as inhomogeneity of model ground and soil structures, unrepeatability of external loading. In ASME's guideline for Verification and Validation (V&V) in computational solid mechanics (2006), uncertainty quantification is clearly necessary for both physical and numerical modeling during V&V process. In this preliminary study, we performed some test cases with the same target experimental conditions through centrifuge modeling for seismic behavior of an embankment on liquefiable ground. We discussed the variation in the seismic responses of embankment with the variations in the materials properties and input acceleration motions.

1 INTRODUCTION

Many numerical methods for geomechanics have been proposed and validated since 1960's. As for static or quasi-static problems such as settlement of embankment on soft clay, in-situ real cases have been good targets of validation for numerical methods. As for dynamic problems such as deformation of liquefied sandy ground, shaking table tests rather than real cases have been good targets because of lack in earthquake motion information in the real cases. For example, in the VELACS project (Arulanandan and Scott 1993 and 1994) some numerical methods with sophisticated constitutive modelling of liquefiable sand under dynamic condition were validated with some centrifuge models and some numerical codes have been successfully applied in practice. Contribution of the VELACS project on the development of numerical modeling on liquefiable ground has never been underrated. Recently after the development of new and innovative models, the LEAP (Liquefaction Experiment and Analysis Projects) (Tobita et al. 2014) re-visited it. A Class A predictions were conducted by numerical models of four institutes for a series of centrifuge experiments of flat and inclined saturated sand deposit.

Figure 1 shows typical comparison between experimental and numerical results of horizontal displacement of liquefied inclined ground from LEAP (Tobita et al. 2014). It looks good agreement; however, they were deterministic and they did not discuss the variations and uncertainties in the experiments and analyses. For example, the numerical results assumed homogeneous ground; however, the experimental model ground were essentially inhomogeneous. Uncertainties in centrifuge modeling have not been discussed in most validation cases of geotechnical problems although it was well known that geotechnical centrifuge modeling includes some uncertainties such as inhomogeneity of model ground and soil structures, unrepeatability of external loading. In ASME's guideline for Verification and Validation (V&V) in computational solid mechanics (2006), uncertainty quantification is clearly necessary for both physical and numerical modeling during V&V process. Following the ASME V&V geotechnical centrifuge modeling and its numerical modeling should discuss uncertainties in the modeling in the future. In this preliminary study as the first step of V&V, we conducted some cases with the same target experimental conditions through centrifuge modeling for seismic behavior of an

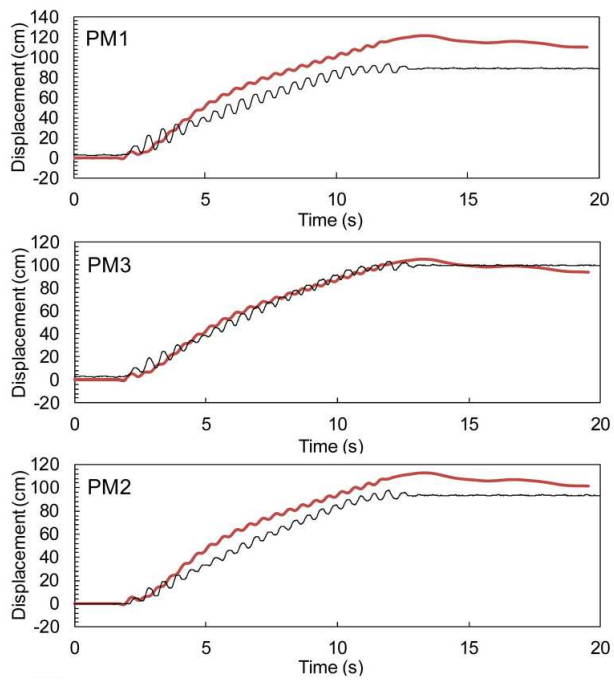

Figure 1. Comparison of experimental (black) and numerical (red) results of horizontal displacement of liquefied inclined ground (from Tobita et al. 2014)

embankment on liquefiable ground. We discussed the variations in the seismic responses of embankment with the variations in the materials properties and input acceleration motions.

2 EXPERIMENTAL CONDITIONS

The centrifugal acceleration was 25G in all experimental cases. This chapter describes the model preparation, test procedures and measurement items in model tests. The dimensions of model are expressed in model scale.

2.1 Model Preparation

Figure 2 shows the model configuration. A foundation ground, saturated embankment and unsaturated embankment were set in a rigid container with the internal dimensions of 375mm long, 175mm wide and 200mm deep. In this study, we focused on deformation and seepage behavior of embankment only, so the foundation ground was made of rigid impermeable cement mortars. A shape of the saturated embankment was reversely trapezoidal form with the depth of 20mm considering of liquefaction at the bottom of embankment (Sasaki et al. 1993, Kaneko et al. 1995, Finn and Sasaki 1997). The material of embankment was mixed sand of Toyoura sand (G_s=2.656, U_c=1.48) and Keisha (silica sand) No.7 (G_s=2.695, U_c=1.74). The weight ratio of Toyoura sand and Keisha No.7 was 8:2. The maximum void ratio, minimum void ratio and maximum dry density of the mixed sand are 0.921, 0.597 and 1.610 g/cm^3 respectively. First, the dry mixed sand of the saturated part was pluviated in air. The target relative density of saturated embankment was 50% (e=0.759, ρ_d=1.460 g/m^3). Second, the unsaturated part was compacted with the target degree of compaction of 80% (e=0.995, ρ_d=1.288 g/m^3). The initial moisture content of unsaturated part was about 13.0%. The dimensions of embankment were 30mm wide at the crest, 65mm high and 290mm wide at the bottom. The inclination of slope was 1:2. The degree of saturation of unsaturated embankment varied from about 60 % to 100 % estimated from the water retention test.

Table 1 shows test cases with initial conditions of embankments. The target of relative density of saturated embankment and the degree of compaction of unsaturated embankment in each test case were set to be the same value, however, the void ratios varied slightly.

2.2 Test Procedures

The procedures in model tests were divided into saturation and shaking processes in centrifugal field. Each process is described in detail as follows.

After the centrifugal acceleration increased in 25G, we supplied pore water from the inlet and made the saturated part saturate in order to reproduce liquefaction in the bottom of embankment. Pore fluid water in the model tests was 25cst methylcellulose considering similitude law. We kept the water level at the height of 5mm from the ground surface by visual observation and by measured values of pore water pressure (CH04 - CH08).

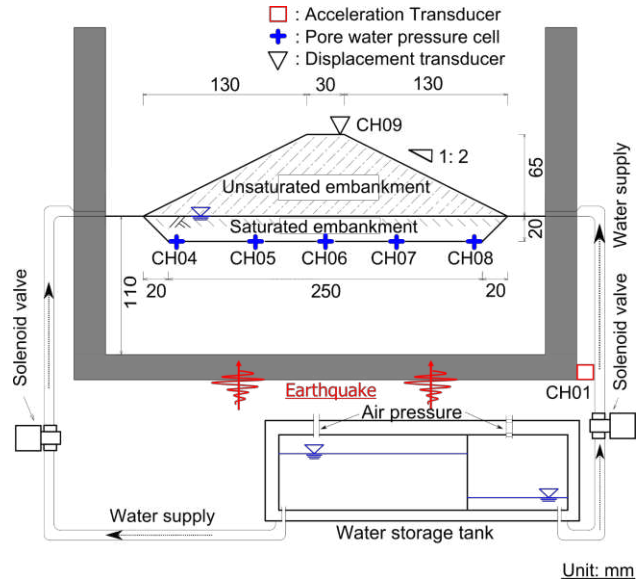

Figure 2. Experimental model configuration

Table 1. Test cases with initial conditions of embankments

Case	Void ratio of saturated part	Void ratio of unsaturated part
1	0.757	1.005
2	0.771	0.990
3	0.763	0.905
4	0.766	0.973
5	0.765	0.971

The water level was adjusted by solenoid valve and air regulator which was set nearby water storage tank. After confirming that pore water pressure became the predetermined value, we drained the water from inlets at both sides of container.

After saturation process, we applied shaking with electronic mortar and camshaft. In all cases, the targets of time duration of shaking, frequency and number of cycles were 1.5 sec, 17 Hz, and 25 cycles respectively. The averaged amplitude of shaking acceleration was about 68 m/s^2.

2.3 Measurements

We measured the crest settlement, excess pore water pressure at the bottom of embankment and input acceleration during shaking tests. Acceleration transducer (CH01) was set on the side of a rigid container in Figure 2 to measure the input acceleration. Pore water pressure cells (CH04 - CH08) were set at the bottom of embankment to measure excess pore water pressure during shaking tests and water level in embankment during saturation process before the shaking tests. Vertical displacement transducer was set perpendicularly at the top of embankment to measure the crest settlement of embankment.

3 EXPERIMENTAL RESULTS

This chapter pr esents the results of shaking tests. All results are expressed in model scale.

Figure 3 shows the side view afte r shaking in all cases. The shaki ng induced lateral deformation near the toe of embankment slope, some cracks on the crest and slope and the crest settlement.

Figure 4 show s the time histories of input acceleration at CH01 . The acceleration histories were slightly different each other although we set the same shaking conditions for all cases.

Figure 5 shows the time histories of crest settlement at CH09. The crest settlements in all cases varied widely although we set the same target conditions for all cases.

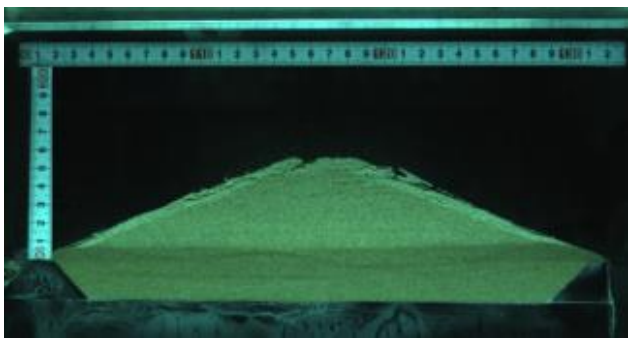

(a) Case 1

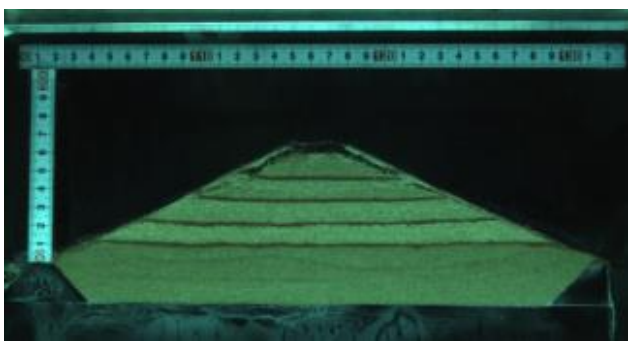

(b) Case 2

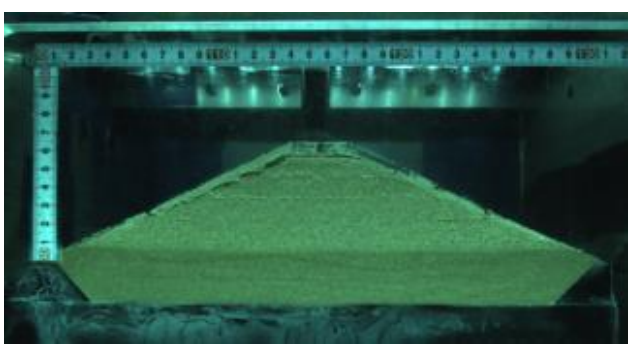

(c) Case 3

Figure 3. Side view of deformed embankment after shaking

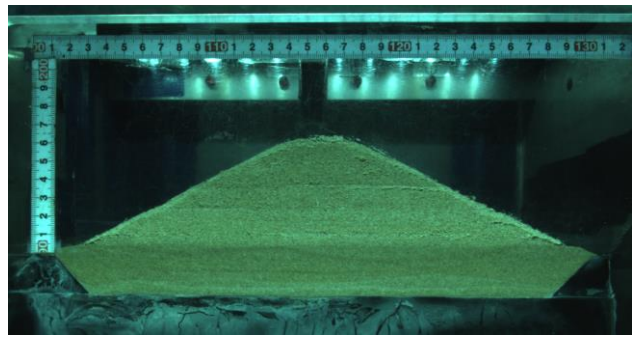

(d) Case 4

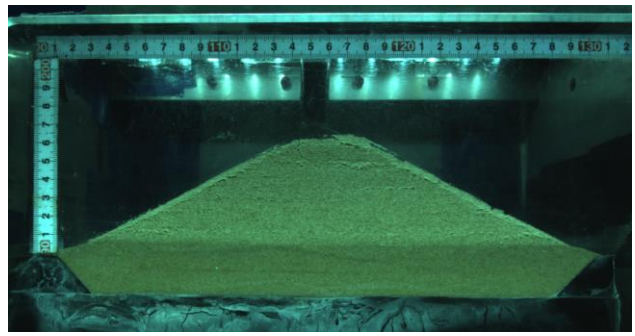

(e) Case 5

Figure 3. Side views of deformed embankment after shaking

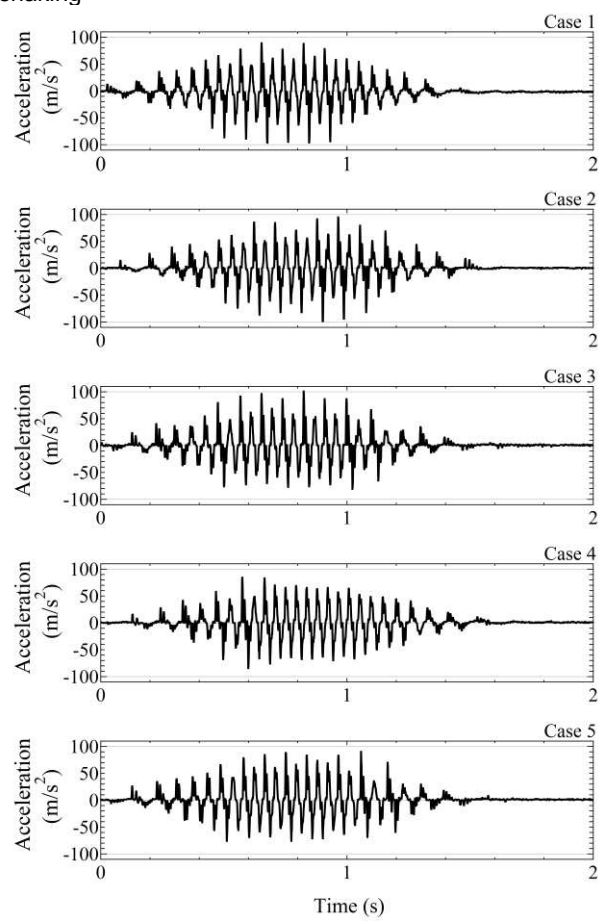

Figure 4. Time histories of input acceleration at CH01

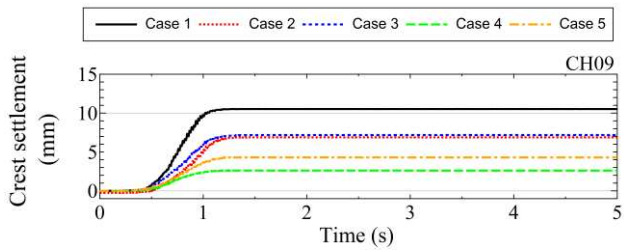

Figure 5. Time histories of crest settlement at CH09

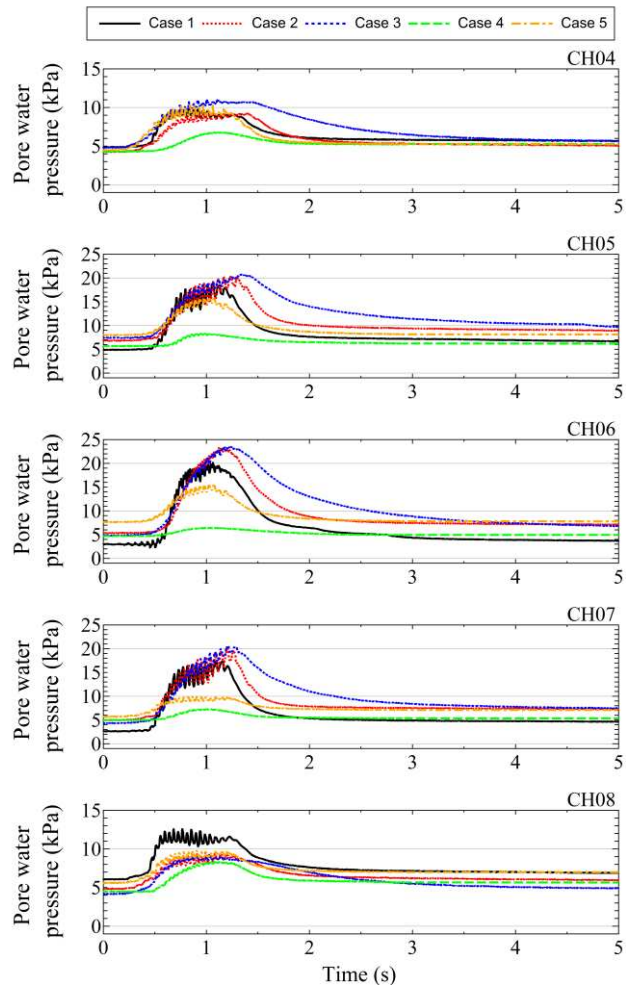

Figure 6. Time histories of pore water pressure at CH04-CH08

Table 2. Crest settlement and averaged input acceleration

Case	Crest settlement (mm)	Averaged input acceleration (m/s^2)
1	10.5	72.8
2	7.1	69.0
3	6.9	67.8
4	2.7	66.0
5	4.4	66.3

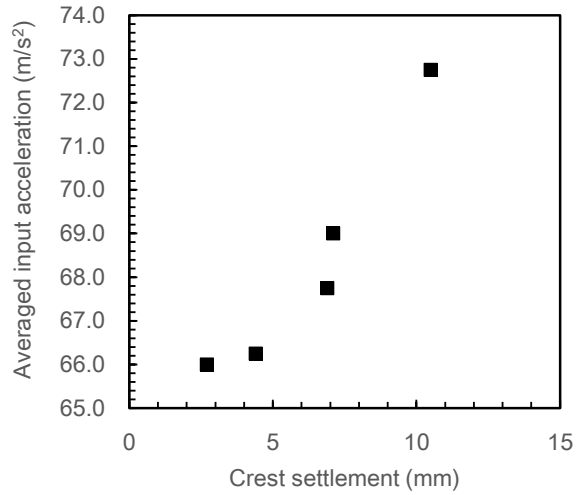

Figure 7. Relationships between crest settlement and averaged input acceleration

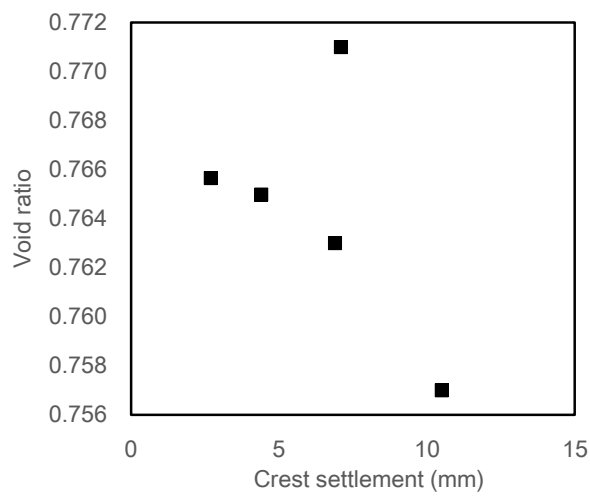

Figure 8. Relationships between crest settlement and void ratio of saturated embankment

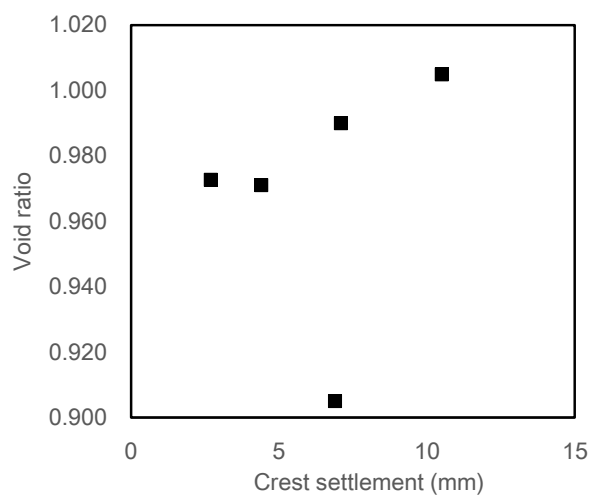

Figure 9. Relationships between crest settlement and void ratio of unsaturated embankment

Figure 6 shows the time histories of pore water pressure at CH04 - CH08. The pore water pressures were the measured pore water pressure before the saturation process; therefore, the initial values varied at some measurement points. It was expected that CH04 - CH08, and CH05 - CH07 showed similar response due to the symmetry; however, the responses were not similar in some cases except for case 2. This asymmetric behavior is possible due to inhomogeneous properties in the saturated embankment. In the cases 4 and 5, the increases of pore water pressure were smaller than other cases; therefore, the small loss of stiffness resulted in small crest settlement. The pore pressure behavior caused smaller crest settlement in the cases 4 and 5.

Table 2 shows the crest settlement after shaking and average input acceleration. The average input acceleration was calculated as the average of absolute peak values of input acceleration wave. The results show that the larger average input acceleration caused the larger crest settlement. Although the same input conditions are set in the all cases, the average input accelerations and crest settlements of Case 1, 2, and 3 were larger than that of Case 4 and 5. It is possible that this difference was due to the conditions such as oil around the camshaft of shaking mechanism.

4 DISCUSSION

Figure 7 shows the relationships between crest settlement after shaking and averaged input motion. As mentioned above the larger average input acceleration caused the larger crest settlement. It is natural that the crest settlement has clear correlation with averaged input motion. Figures 8 and 9 show the relationships between crest settlements after shaking and void ratio of saturated and unsaturated embankment respectively. There are no clear correlations between crest settlements after shaking and void ratios of saturated and unsaturated embankment. In these experimental conditions, the variations in the averaged input acceleration had more effect on the crest settlement than that in the void ratios of embankment. The crest settlement of the embankment under a shaking can be a result of different factors including the liquefaction-induced migration of underlying soil toward the embankment toe, shear deformation of the embankment, and contractive volume change of the soil foundation and the embankment. Unfortunately, we could not measure the degree of saturation of the unsaturated embankment before and after shaking. We need further investigation on different factors.

Figure 10 shows the histograms of crest settlement after shaking, void ratios of saturated and unsaturated embankment. The average crest settlement was 6.32 mm, and the standard deviation was 1.33 mm. The average void ratio of saturated embankment was 0.764, and the standard deviation was 0.002. The average void ratio of unsaturated embankment was 0.969, and the standard deviation was 0.017. The scatter in the crest settlement is larger than that in the void ratios. However we performed only five cases in this study; therefore, it was difficult to analyze reliable statistics. We need more cases to discuss the uncertainties of experimental results.

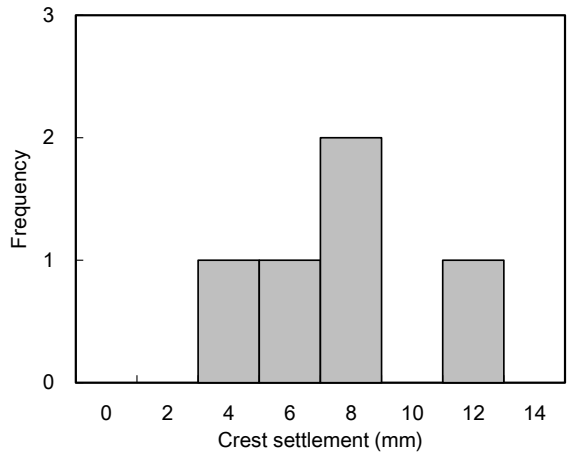

(a) Crest settlements

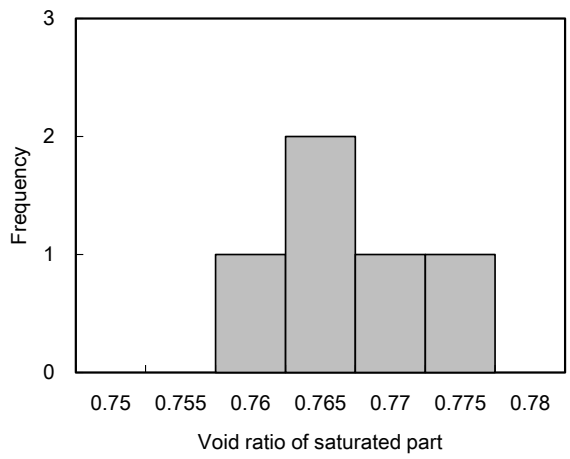

(b) Void ratio of saturated embankment

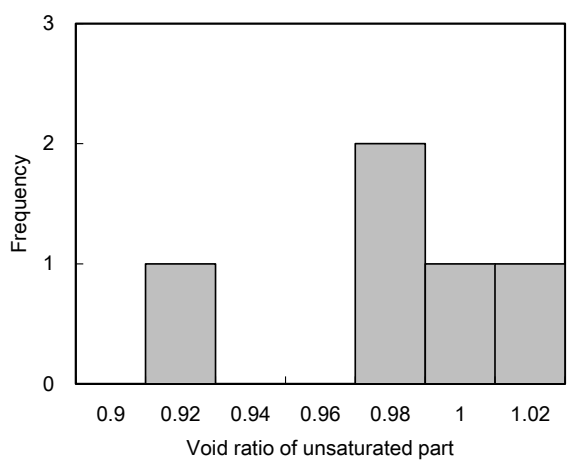

(c) Void ratio of unsaturated embankment

Figure 10. Histograms

5 CONCLUSIONS

In this preliminary study as the first step of V&V, we performed some test cases with the same target experimental conditions through centrifuge modeling for seismic behavior of an embankment on liquefiable ground. We discussed the variations in the seismic responses of embankment with the variations in the materials properties and input acceleration motions, and crest settlements after shaking. In these experimental conditions, the variations in the averaged input acceleration had more effect on the crest settlement than that in the void ratios of embankment. It seems that the variations in the averaged input acceleration was too large due to unexpected shaking mechanical problems. We need further investigation of repeatability of shaking and more cases to discuss the uncertainties of experimental results.

ACKNOWLEDGEMENTS

This work was supported by JSPS KAKENHI Grant Number JP 16H04409. The authors thank Mr. Kei Ito and Mr. Kohei Hara for their work in the centrifuge experiments.

REFERENCES

The American Society of Mechanical Engineers. 2006. *ASME V&V 10-2006 Guide for Verification and Validation in Computational Solid Mechanics*, ASME, New York, NY, USA.

Arulanandan, K. and Scott, R.F. 1993 and 1994. Verification of Numerical Procedures for the Analysis of Soil Liquefaction Problems. *Proceedings of the international conference on the Verification of Numerical Procedures for the Analysis of Soil Liquefaction Problems*, Vols. 1 and 2. A. A. Balkema, Netherlands.

Finn, W. and Sasaki, Y. 1997. Simulation of response of the Kushiro river dike to the 1993 Kushiro-oki and 1994 Hokkaido Toho-oki earthquakes, *14th International Conference on Soil Mechanics and Foundation Engineering*, 99–102.

Kaneko, M., Sasaki, Y., Nishikawa, J., Nagase, M. and Mamiya, K. 1995. Ri ver dike failure in japan by earthquakes in 1993, *Third International Conference on Recent Advances in Geotechnical Earthquake Engineering and Soil Dynamics*, 495-498.

Sasaki, Y., Oshiki, H. and Nishikawa, J. 1993. Embankment failure caused by the Kushiro-oki earthquake of January 15, *Performance of Ground and Soil Structure during Earthquakes, 13th International Conference on Soil Mechanics and Foundation Engineering*, 61–68.

Tobita, T., Manzari, M.T., Ozutsumi, O., Ueda, K., Uzuoka, R., Iai, S. 2014. Benchmark centrifuge tests and analyses of liquefaction-induced lateral spreading during earthquake, *Geotechnics for Catastrophic Flooding Events - Proceedings of the 4th International Conference on Geotechnical Engineering for Disaster Mitigation and Rehabilitation*, GEDMAR 2014, Iai, S. (Ed), Kyoto, 127-182.